Trends in Evaporation of a Large Subtropical Lake

Cheng Hu[1,2], Yongwei Wang[1], Wei Wang[1], Shoudong Liu[1], Meihua Piao[1,3], Wei Xiao[1], Xuhui Lee[1,4]

1: Yale-NUIST Center on Atmospheric Environment, Nanjing University of Information Science and Technology, Nanjing 210044, China

2: Collaborative Innovation Center of Atmospheric Environment and Equipment Technology, Nanjing University of Information Science and Technology, Nanjing 210044, China

3: Jilin Meteorological Bureau, Jilin 130062, China

4: School of Forestry and Environmental Studies, Yale University, New Haven, Connecticut 06511, USA

Corresponding author:

Xuhui Lee
Sara Shallenberger Brown Professor of Meteorology
School of Forestry and Environmental Studies
Yale University
New Haven, CT 06511, USA
Email: xuhui.lee@yale.edu

Revision submitted to *Theoretical and Applied Climatology*
(January 30, 2016)

Abstract

How rising temperature and changing solar radiation affect evaporation of natural water bodies remains poor understood. In this study, evaporation from Lake Taihu, a large (area 2400 km^2) freshwater lake in the Yangtze River Delta, China, was simulated by the CLM4-LISSS offline lake model and estimated with pan evaporation data. Both methods were calibrated against lake evaporation measured directly with eddy covariance in 2012. Results show a significant increasing trend of annual lake evaporation from1979 to 2013, at a rate of 29.6 mm $decade^{-1}$ according to the lake model and 25.4 mm $decade^{-1}$ according to the pan method. The mean annual evaporation during this period shows good agreement between these two methods (977 mm according to the model and 1007 mm according to the pan method). A stepwise linear regression reveals that downward shortwave radiation was the most significant contributor to the modeled evaporation trend, while air temperature was the most significant contributor to the pan evaporation trend. Wind speed had little impact on the modeled lake evaporation but had a negative contribution to the pan evaporation trend offsetting some of the temperature effect. Reference evaporation was not a good proxy for the lake evaporation because it was on average 20.6% too high and its increasing trend was too large (56.5 mm $decade^{-1}$).

Key words: global warming, lake evaporation, eddy covariance, lake model

1 Introduction

There are 304 billion lakes in the world, occupying more than 3% of the continental land surface (Downing et al., 2006). Evaporation from these lakes plays a vital role in the global energy distribution and the hydrological cycle (Torcellini et al., 2004; Fu et al., 2004; Subin et al., 2012a; Rong et al., 2013). There are several methods for quantifying lake evaporation. The water balance method determines the lake evaporation from precipitation and the amounts of water that flow in and out of the lake. The energy balance method derives the evaporation rate by distributing the available energy to sensible heat and latent heat fluxes (Rosenberry et al., 1993; Winter et al., 1995; Rosenberry et al., 2007; Elsawwaf et al., 2010). The pan coefficient method estimates lake evaporation from pan evaporation data collected in the lake catchment using a pan coefficient which is the ratio of pan evaporation to actual lake evaporation (Hoy and Stephens et al., 1977; Jensen et al., 1990; Abtew et al., 2001; McJannet et al., 2013). Lake evaporation can also be calculated with sophisticated lake models based on physical processes of energy transfer in the lake and between the lake and the atmosphere (Dutra et al., 2010; Subin et al., 2012a). Finally, the eddy covariance (EC) technique is increasingly used to measure temporal and spatial variations in evaporation and energy fluxes of lake systems (Blanken et al., 2000; Liu et al., 2009; Nordbo et al., 2011; Lee et al., 2014). Most of the EC studies are limited in duration, and long-term (> 10 years) trend analysis is still not feasible with this method. Each of these methods has its strengths and weaknesses. A combined use of multiple methods may lead to more robust assessment of lake evaporation trends than using a single method alone.

IPCC (2013) reported that the global average air temperature has risen by 0.7 °C from

1951 to 2012. Questions remain as to how lake evaporation has changed in this period and whether the evaporation trends are a good proxy indicator of the impact of rising temperature on the global hydrological cycle (Xu et al., 2006; Williamson et al., 2009). This debate is sometimes framed as the “evaporation paradox”, the phenomenon in which pan evaporation has decreased globally in the past 50 years (Peterson et al., 1995; Chattopadhyay and Hulme et al., 1997; Brutsaert et al., 1998; Roderick et al., 2002; Cong et al., 2009), contrary to the belief that higher temperature should accelerate the hydrologic cycle. Most of previous studies about the effect of global warming on evaporation and on the “evaporation paradox” rely on data on land potential evapotranspiration, pan evaporation and reference evapotranspiration. Three explanations are offered for the paradox: 1) the increasing temperature leads to higher actual evaporation on land, which weakens ability for the atmosphere to take up water vapor from standing water surfaces due to enhanced air humidity; 2) Decreasing wind speed causes the decrease in pan evaporation (Roderick et al., 2007); 3) “Global dimming”, or the decrease in sunshine duration and incoming radiation, causes the decrease in pan evaporation (Roderick et al., 2002).

The global dimming explanation emphasizes the important role of solar radiation energy in controlling evaporation. For example, Rong et al. (2013) combined the Penman-Monteith model with reference evaporation data to calculate the annual evaporation of Dongping Lake in Northern China, and concluded that from 2003 to 2010, the annual evaporation increased at the rate of 18.24 mm year^{-1}, and increasing solar radiation and temperature explained this increasing evaporation trend. Using the energy budget method to calculate evaporation from Sparking Lake in open-water seasons (May-November, from 1989 to 1998), Lenters et al.

(2005) reported that the lake evaporation decreased from 1989 to 1994 and then continued rebounding to a higher value in 1998, following similar variations in net radiation.

Some studies have showed that the decreasing trend in the incoming solar radiation was reversed to an increasing trend in the late 1980s, but the pan evaporation continues to decrease (Pinker et al., 2005; Wild et al., 2005), suggesting that factors other than solar radiation may also play large roles. Johnson and Sharma (2010) estimated that the evaporation of open waters should increase by 7% from 1990 to 2070 under the SRES A2 climate scenario, concluding that rising temperature is one potential contributor to the rising trend. Zhu et al. (2010) evaluated the evaporation trend of Nam Co Lake on the Tibetan Plateau by using remotely sensed lake area and a reference evaporation model; they concluded that this lake was increasing in size due to increasing glacier melt, but paradoxically the rate of evaporation showed a decreasing trend despite a robust increasing trend in air temperature. The lack of consistent trends under conditions of increasing temperature may be an indication that these proxy evaporation data are not an accurate representation of the actual lake evaporation or that air humidity and wind speed effects may more than offset the temperature effect.

The objective of this study is to investigate the long-term evaporation trend and the underlying mechanisms for Lake Taihu, a large (area 2400 km^2) and shallow (depth 1.9 m) lake in the Yangtze River Delta, China. Average air temperature in the Lake Taihu catchment increased by 1.62°C from 1961 to 2009, at a rate more than twice as the global average (IPCC 2013), and annual mean wind speed decreased significantly from 3.45 to 2.44 m s^{-1} in the same period. The surface solar radiation increased by 8.3 W m^{-2}, or roughly 6%, from

1979 to 2013. These unambiguous and yet opposing atmospheric changes provide a unique opportunity for generating new insights into the evaporation paradox. We employed pan evaporation data and a lake land-surface model coupled to atmospheric reanalysis to calculate the annual lake evaporation. Both methods were calibrated against the direct measurement of the lake evaporation via eddy covariance. The calibrated methods should provide a more robust assessment of trends and interannual variabilities than proxy data (uncorrected pan evaporation, reference evaporation). The specific goals of this study are: 1) to quantify the annual Lake Taihu evaporation trend; 2) to determine if this trend can be explained by temperature, wind and solar radiation variability; 3) to investigate whether reference evaporation can be used as proxy for determining the lake evaporation trend.

2 Materials and Methods

2.1 Study site

Lake Taihu (30°5’40’’- 31°32’58’’N and 119°52’32’’-120°36’10’’E; Figure 1) is located in the Yangtze River Delta, China. The perennial surface area is 2400 km^2 and the average depth is 1.9 m. The lake is in the Asian monsoon climate zone, with an annual average temperature of 15.97°C and annual rainfall of 1182 mm (1961-2009). The elevation is about 3 m above the sea level.

2.2 Eddy covariance observation

Eddy covariance measurement of the lake evaporation at two locations in the lake, one near the west shore (Dapukou, or DPK) and the other in the eastern portion of the lake

(Bifenggang, or BFG), was used in this study (Figure 1). Both sites have excellent fetch. These sites are part of the Taihu Eddy Flux Network (Lee et al. 2014). Details of the instrumentation are described by Lee et al. (2014). Small data gaps were filled with the bulk transfer relationships (Garratt et al., 1992; Laird and Kristovich et al., 2002; Wang et al., 2014). The original half-hourly data were averaged to 5-day intervals and adjustment was made to the sensible and latent heat flux by forcing energy balance closure (Twine et al., 2000). The adjusted latent heat flux was then used to validate the lake model and to calibrate the pan evaporation data, as described below.

2.3 The lake land-surface model

We used the CLM-LISSS (National Center for Atmospheric Research Community Land Model version 4- Lake, Ice, Snow and Sediment Simulator) lake model to calculate lake evaporation (Subin et al. 2012b). CLM-LISSS is an improved version of CLM4-Lake (Bonan et al., 1995; Zeng et al., 2002). It parameterizes the heat diffusion in the water column with a bulk eddy diffusivity formulation and solves the lake surface temperature from the surface energy balance equation. The latent and sensible heat fluxes are calculated from the bulk transfer relationships. The main forcing variables are net shortwave radiation flux, downward longwave radiation flux, wind speed at the 10-m height, and specific humidity and air temperature at the 2-m height. Recently, our group (Deng et al., 2013) evaluated the model against the eddy covariance observations at Lake Taihu. We found that the model does a good job simulating the eddy fluxes and the water temperature after an adjustment has been made to the water thermal diffusivity parameterization. In this study, we used the version tuned by

Deng et al. (2013).

The CLM4-LISSS lake model was forced by MERRA (The Modern-Era Retrospective Analysis for Research and Applications) data. MERRA is an atmospheric reanalysis system developed by NASA using the Goddard Earth Observation Model (Rienecker et al., 2011). The reanalysis dada covers the period from 1979 until now. The model grid resolution is 1° by1.25° for the surface downward shortwave radiation ($S_{\downarrow}$), the surface upward shortwave radiation ($S_{\uparrow}$), and the surface downward longwave radiation data ($L_{\downarrow}$), and 1/2° by 2/3° for specific humidity, wind speed, air temperature and pressure. The radiation data used for this study came from the grid centered at 31.5°N and 120.63°E and the standard meteorological variables from the grid centered at 31.5°N and 120.0°E. The forcing variables from MERRA are surface pressure, air temperature, specific humidity, wind speed, downward shortwave radiation and downward longwave radiation at 3-hourly intervals. The upward shortwave radiation was calculated from the downward shortwave radiation and the observed lake albedo of 0.08.

Previous studies have shown that the MERRA $S_{\downarrow}$ is biased high by around 20 Wm^{-2} when compared with FLUXNET observations in North America and Atmospheric Radiation Measurement Program in the Southern Great Plains (Zhao et al., 2013; Kennedy et al., 2011). Its surface downward longwave radiation is biased low by 19 Wm^{-2} (Kennedy et al., 2011). We found that MERRA overestimated the annual mean $S_{\downarrow}$ by 38.4 Wm^{-2}, and underestimated the annual mean $L_{\downarrow}$ by 26.2 Wm^{-2} in comparison to the observations at Lake Taihu in 2012.

To eliminate these biases, we used a simple linear fitting method for $S_{\downarrow}$ and $L_{\downarrow}$ by establishing a regression equation of the 3-hour means of the MERRA outputs against the observed values. We established the correction coefficients using the data in 2012 and assessed the accuracy of the regression fits for 2013. After the correction, the mean annual biases of $S_{\downarrow}$ and $L_{\downarrow}$ were reduced to 4.8 W m^{-2} and 1.6 W m^{-2}, respectively. The corrected $S_{\downarrow}$ shows very good agreement, in terms of long-term trends and interannual variabilities, with observations made in Shanghai (31.1°N, 121.3°E), about 90 km to the east of the lake.

We applied a similar method to calibrate other MERRA variables. After calibration, the mean bias in the MERRA specific humidity came down from 0.000724 kg kg^{-1} (relative error 7%) to 0.000034 kg kg^{-1} (relative error 0.3%). The mean wind speed was underestimated by 0.54 m s^{-1} for the year of 2012, after the calibration, the mean bias decreased from 0.53 to 0.015 m s^{-1} for the validation year of 2013. The mean daily air temperature from MERRA and lake show small biases (mean error 0.90°C, root mean squares error 1.96°C). To correct these biases, we established linear regression for each month of the year. The corrected air temperature had improved accuracy (mean error 0.25°C, root mean squares error 1.30°C).

2.4 Pan evaporation

Pan evaporation data were obtained from eight sites near the lake (Figure 1; Table 1). Two of the sites covered continuously the period from 1971 to 2013, and four sites covered continuously the period from 1961 to 2013. The E601 pan (61.8 cm in diameter), a modified type of GGI-3000, a standard evaporation pan recommended by the World Meteorological Organization, was used at four sites (Dongshan, Changshu, Huzhou, Wuxi). The Φ20 pan (20 cm in diameter) was used at the other four sites (Changshu, Yixing, Jintan, Wujiang).

2.5 Reference evaporation

Reference evaporation has been used frequently in the studies of evaporation trend in the terrestrial environment. To test whether reference evaporation is a good proxy for the evaporation trend for Lake Taihu, we presented below a comparison of reference evaporation with the pan evaporation data and the model results. Reference evaporation for Lake Taihu (ET_0) was calculated using the Penman-Monteith model (Allen et al., 1998), assuming a hypothetical reference grass whose height is 0.12 m, surface resistance is 70 s m^{-1} and albedo is 0.23. In the model, the net radiation is computed as a function of sunshine duration and water vapor pressure, and soil heat storage is computed as a function of difference in air temperature between two consecutive days. Input variables include daily air temperature (maximum, minimum and average), wind speed, relative humidity, and sunshine duration; these data came from actual observations made at the weather stations near the lake (Figure 1). Details of all the data needed for the calculation of ET_0 are given in Chapter 3 of FAO paper 56 (Allen et al., 1998).

2.5 Statistical analysis

A multiple stepwise regression method was employed to analyze the effect of each independent variable on the trends of evaporation. These variables were normalized between 0 and 1, with 0 corresponding to the minimum value and 1 to the maximum value. A variable was entered in the model if its initial *p* value was less than 0.05 and was removed if the recalculated p value was larger than 0.1. The contribution of each variable to the lake evaporation trend was calculated as follows:

$$Y = a_1X_1 + a_2X_2 + a_3X_3 \ldots \quad (1)$$

$$\mu_i = \frac{a_i \Delta X_i}{\Delta Y} \quad (2)$$

where Y is the normalized dependent variable (annual mean lake evaporation), X_i (i = 1, 2, 3,…) are the normalized independent variables, a_i is the regression coefficient for variable X_i, μ_i is the actual contribution of X_i to Y, and ΔX_i and ΔY are the trends of X_i and Y which are the product of their slope of linear regression against the time span (Xu et al., 2006; Wang et al., 2007). The dependent variable was either modeled annual evaporation, adjusted annual pan evaporation, or annual reference evaporation. Normalization of the variables was made with their maximum and minimum values so that after normalization they varied in the range of 0 to 1. Because all the variables are normalized, the regression coefficients are dimensionless.

In the case of modeled lake evaporation, the MERRA annual mean air temperature, wind speed, downward longwave radiation, downward shortwave radiation, precipitation and specific humidity were used as independent variables. Their linear time trends are shown in Figure 2. The MERRA air temperature, incoming solar radiation, humidity, air temperature and precipitation time trends are in excellent agreement with the station data. However its wind speed shows a statistically insignificant trend, whereas the station observations indicate a significant downward trend. So we also did a second set of stepwise regression by replacing the reanalyzed wind speed with the observed value but using the reanalysis for all other independent variables. No station observation was available for comparison with the MERRA incoming longwave radiation.

3 Results and Discussion

3.1 Results of the CLM4-LISSS lake model

The modeled latent heat and sensible heat flux show excellent agreement with the EC observation (Figure 3). Here the lake model was run twice, once forced by in-situ meteorological observations at the BFG site and the second time forced by the calibrated MERRA forcing variables. The 3-hourly model outputs of latent heat and sensible heat fluxes were averaged over 5-day periods for comparison with the observation. If the model was forced with in-situ observations, the mean error and the RMSE of the 5-day mean latent heat flux were 0.4 Wm^{-2} and 16.7 Wm^{-2}, respectively. If the model was forced with the MERRA meteorology instead, the model performance was slightly degraded, with the mean error of 0.6 Wm^{-2} and RMSE of 27.3 Wm^{-2} (Table 2).

The annual and seasonal variations of modeled evaporation from Taihu are plotted in Figures 4 and 5. In the last three years (2011-2013) of the study period, the modeled annual evaporation rate and trend were in excellent agreement with the values observed with EC at DPK (Figure 5). We used the data from the DPK eddy covariance site because it had longer and more continuous measurements than at BFG. The modeled evaporation rate is also in excellent agreement with the pan-adjusted evaporation rate (Figure 5), with a linear correlation coefficient of 0.79 ($p < 0.01$).

Use of a constant albedo and reanalyzed incoming longwave radiation are likely to be the two largest sources of error. Lake albedo is known to vary with the optical depth of aerosols in the atmosphere, cloudiness, solar zenith angle, and wind speed (Katsaros et al., 1985; Henneman et al., 1999). Some of the scatters seen in the short-term flux comparison (Figure 3) may have been caused by the albedo variability. But averaged over the annual cycle, these scatters seem to have canceled out, resulting in good agreement with the observations (Figure 5). Reanalysis models have a tendency to underestimate the incoming longwave radiation (Kennedy et al., 2011). The good agreement with the eddy-covariance annual evaporation rate for the calibration year (2012) as well as the other years (2011, 2013, 2014) indicates that the above empirical adjustment to $L_{\downarrow}$ was robust.

According to the model calculation, Lake Taihu's annual evaporation increased significantly at a rate of 29.6 mm decade^{-1} from 1979 to 2013 (the standardized MK (Mann et al., 1945; Kendall et al., 1975) statistic z = 2.83, 99% confidence level). Using meteorological observations and combining the Penman-Monteith equation and a reference evaporation ratio algorithm, Rong et al. (2013) showed an increasing trend of Dongping Lake, which is 640 km northwest of Lake Taihu, at a rate of 4.55 mm year^{-1} from 2003 to 2010 and concluded that rising air temperature and net radiation accounted for the increase. The global evapotranspiration of land showed an increasing trend at the rate of 7.1 mm decade^{-1} from 1982 to 1997 (Jung et al., 2010). Based on a water balance analysis, increasing trend of actual evapotranspiration of six large basins (Mississippi, Sacramento, Susquehanna, Colorado, Columbia, and Southeast) in the conterminous USA was reported between 1950 and 2000 (Walter et al., 2004). However, Baker et al. (2012) found that most of watersheds in Minnesota, USA displayed a decreasing trend in evapotranspiration over the past three decades.

When taking the 35 years as a whole, the lake evaporation shows increasing trends in all the four seasons but with different magnitudes. The rate of increase for spring, summer, autumn, winter was 14.7, 9.2, 4.8 and 0.9 mm decade^{-1}, respectively. The average annual evaporation for the period from 1979 to 2013 was 977 mm, and varied in the range between 889 mm in 1985 and 1138 mm in 2013. From the results of the MK test, the increasing trend was significant for the annual and the spring period (z = 2.82 for annual and 3.48 for spring, 99% significance level), was marginal for the summer period (z = 1.98, 90% significance level), and did not past the significance test for the winter and autumn seasons (z = 0.58 for winter and 1.35 for autumn).

To determine factors that contributed to the increasing trend of annual evaporation, we first analyzed the trends of the MERRA forcing variables, including the screen-height air temperature (T), and specific humidity (q), 10-m wind speed (U), downward longwave radiation ($L_{\downarrow}$), downward shortwave radiation ($S_{\downarrow}$) and precipitation (P) (Figure 2). Two variables, T and $S_{\downarrow}$ increased significantly, at the rate of 0.34°C decade^{-1} and 1.91 W m^{-2} decade^{-1} (99% confidence level). The downward longwave flux increased slightly, at a rate of 0.63 W m^{-2} decade^{-1} (90% confidence level). The other variables (q, P, U) showed no significant trends. The temporal trends in the MERRA variables, $S_{\downarrow}$, T, q and P, are in good agreement with actual observations on land, but the lack of trend in the MERRA wind speed contradicts with the observed wind in the Lake catchment showing a declining trend of 0.12 m s^{-1} decade^{-1} (99% confidence level). Additionally, the lower observed wind speed than the MERRA wind speed can be explained by the fact that wind on land is weaker than wind over the open lake, keeping in mind that the MERRA wind data were calibrated against the wind observations over the lake. No observational data on $L_{\downarrow}$ are available for comparison with the MERRA data.

Next, quantitative analysis of the contribution of each independent variable was performed with the stepwise multiple regression method described in Section 2.5. The results are shown in Table 3. The multiple regression coefficients are 0.677, 0.234, 0.219, -0.379 and 0.133 for $S_{\downarrow}$, T, $L_{\downarrow}$, q and U, respectively. Annual precipitation (P) was removed from the regression equation because the recalculated p value was larger than 0.1. The R^2 (coefficient of determination) of the final equation is 0.955, which means that the equation explains 95.5% of the variance in the lake evaporation. The increase of $S_{\downarrow}$ is the most important factor that contributes to 60.9% of the total lake evaporation increase. The second largest contribution comes from T with a percentage contribution of 28.9%. Ranking third and fourth are $L_{\downarrow}$ (10.1%) and q (-5.1%). The contribution by U is very small, at 0.8%. The sum of all the contributions from these independent variables explains 95.6% of the total evaporation increase. In short, at Lake Taihu, increasing downward shortwave radiation is the key contributor to the increased annual evaporation from 1979 to 2013.

Since the wind speed trend differs between MERRA and the actual observation, an additional stepwise regression was performed by replacing the MERRA wind with the observed wind but keeping other MERRA inputs invariables. The results are shown in the bottom portion of Table 3. Interestingly, the wind speed was excluded from the final regression because its recalculated p value was greater than 0.1. Also excluded were P, $L_{\downarrow}$, and q. Of the two variables remaining, $S_{\downarrow}$ and T contributed 68.5% and 33.8% to the evaporation trend.

The insensitivity to wind speed is consistent with theoretical expectation of open water evaporation. According to the Priestley-Taylor model (Priestley and Taylor, 1972), open water evaporation is controlled by the available energy and temperature and is independent of wind speed. Parameter analysis with the CLM4-LISSS lake model indicates that the surface temperature of Lake Taihu is insensitive to wind (Deng et al. 2013). In the present study, increasing the MERRA wind speed by 10% changed the mean evaporation rate only slightly, by 0.4% to 981 mm from the original mean of 977 mm. That the evaporation rate is nearly identical at two EC sites in Lake Taihu whose wind speed differs by almost a factor of two (Wang et al. 2014) is further evidence supporting the theoretical expectation.

3.2 Trends in pan evaporation

The comparison of pan evaporation to the EC-observed lake evaporation is shown in Figure 6 for the eight pan evaporation sites. The Φ20 pan data are on the left (panels a-d) and E601 pan data are on the right of this plot (panels e-h). Each data point represents a 5-day period. The pan coefficient (the slope of the linear regression) of the four Φ20 pans is smaller than that of the four E601 pans, which means that the annual evaporation is greatest for the Φ20 pans, the lowest for the E601 pans, and actual lake evaporation falls in between these two measurements. Being larger in surface area, E601 pans provided more accurate estimate of the lake evaporation: the mean pan coefficient for E601 is slightly greater than unity (1.11) whereas the mean pan coefficient for Φ20 deviates much more from unity (0.75). In the following, we corrected the historical pan evaporation by multiplying the observed values with the pan coefficient established for each of the pan stations shown in Figure 6.

The adjusted pan evaporation results show an increasing trend from 1979 to 2013, at the rate of 25.4 mm decade^{-1} which is very close to the rate of 29.6 mm decade^{-1} modeled by CLM4-LISSS. In this comparison, the pan evaporation data came from six stations (Changshu, Yixing, Jintan, Dongshan, Changshu, and Huzhou). The Wujiang and Wuxi stations have a data gap of more than five years and have been removed from the calculation. The mean annual evaporation (1979-2013) is 1007 mm according to the pan data and 977 according to the model. The interannual variabilities of the two time series are highly correlated as noted above.

The stepwise regression reveals a dominant role of air temperature in the observed pan evaporation variations (Table 4). In this regression, all independent variables except the incoming longwave radiation came from the station observations. The observed T in the lake catchment contributed 174.5% to the observed pan evaporation trend. The role of $S_{\downarrow}$ is much smaller than for the modeled lake evaporation, with a contribution of 17.3%. These positive contributions were offset by negative contributions from the observed wind (-66.6%) and from the MERRA incoming longwave radiation (-26.6%), bringing the total contribution to slightly over 100% (105.8%).

The negative contribution of the observed wind to the pan evaporation trend is consistent with the “stilling” phenomenon reported by other pan evaporation studies (Roderick and Farquhar, 2006; Rayner et al., 2007) and is supported by a theoretical study on the energy balance of evaporation pans (Lim et al., 2012). However, the lack of wind sensitivity of open-water evaporation suggests that the “stilling” phenomenon may be a consequence of strong horizontal advective effects associated with small surface area of evaporation pans and may not be applicable to large natural water bodies.

3.3 Trends in reference evaporation

Annual reference evaporation ET_0, averaged of the eight pan evaporation sites around Lake Taihu (Figure 1), shows an increasing trend, at a rate of 56.5 mm decade^{-1}, from 1979 to 2013. The sign of the trend is in agreement with the model and the pan data, and is consistent with the study by Brutsaert and Parlange et al., (1998) who concluded that at places with ample supply of moisture, ET_0 can be treated as an indicator of local actual evaporation. The interannual variations in ET_0 are correlated with those in the pan evaporation (linear correlation $r = 0.81$, $p < 0.01$) and in the modeled lake evaporation ($r = 0.75$, $p < 0.01$). However, the long-term mean ET_0 (1197 mm) is 18.9% and 22.5% higher than the pan and the lake evaporation rate, respectively. Also notable is that the rate of increase in ET_0 is 122% and 91% larger than those of the pan evaporation and the lake evaporation, respectively. If we accept the interpretation that ET_0 trends are indicative of how terrestrial ecosystems would respond to climatic changes, our result implies that Lake Taihu, and perhaps other open water bodies as well, are less sensitive to these changes. The stepwise regression reveals that the ET_0 trend was overwhelmingly controlled by the temperature trend (Table 5). The contributions of solar radiation and wind speed were not significant.

Whether long-term evaporation trends are positive or negative appears to depend on the choice of study period. Several previous studies concluded that pan evaporation, land actual evaporation and reference evaporation of the Yangtze River Basin, where Lake Taihu is located, show decreasing trend with the rate of -30.9 mm decade^{-1}, -3.6 to -9.3 mm decade^{-1}

and -19 mm decade^{-1}, respectively, from 1961 to 2000 (Xu et al., 2005; Wang et al., 2007). These authors attributed the decreasing trends to the decreases of net total radiation and wind speed during their study period, even though air temperature increased at the rate of 0.1 °C decade^{-1}. Cong et al., (2009) found that pan evaporation, taking China as a whole, shows a decreasing trend from 1965 to 1985 due to decreasing radiation and wind speed, and an increasing trend from 1986 to 2005, which they attributed to a increasing trend in the vapor pressure deficit.

4 Conclusions

The lake evaporation modeled by CLM4-LISSS is in excellent agreement with eddy covariance observations. The modeled lake evaporation and the calibrated pan evaporation show increasing trend at a similar rate of 29.6 mm decade^{-1} and 25.4 mm decade^{-1}, respectively, from 1979 to 2013. The annual mean lake evaporation was 977 mm according to the model and 1007 mm according to the pan data. The largest contributor to the increasing trend of modeled evaporation was increasing solar radiation during this period, while the largest contributor to the observed pan evaporation trend was increasing air temperature. The decline in the observed wind speed during this period had little impact on the modeled lake evaporation but contributed negatively to the pan evaporation trend.

In the Lake Taihu catchment, reference evaporation ET_0 is not a good proxy indicator of lake evaporation. Although the interannual variations in the annual ET_0 were highly correlated with the modeled lake evaporation and the adjusted pan evaporation, its increasing trend was too strong, at a rate of 56.5 mm decade^{-1}. This trend was overwhelmingly controlled by the temperature trend.

Although the results from the two different methods (model and pan) show an increasing trend in the lake evaporation at similar rates in the past 34 years, they disagree in the main contributors to the observed trend. We argue that the modeled result gives a more robust attribution of climatic impacts on the lake hydrological cycle.

Reference evaporation is expected to be approximately equal to actual evaporation under conditions of ample water supply. However, we conclude that reference evaporation is not a good proxy for lake evaporation study.

Acknowledgements: This research was supported by National Natural Science Foundation of China (Grant 41275024 and 41475141), the setup Foundation for Introducing Talent of Nanjing University of Information Science & Technology (Grant no. 2014r046), the Ministry of Education of China under Grant PCSIRT, and the Priority Academic Program Development of Jiangsu Higher Education Institutions.

References

Abtew, W. (2001). Evaporation estimation for Lake Okeechobee in south Florida. *Journal of Irrigation and Drainage Engineering*, *127*(3), 140-147.

Allen, R. G., Pereira, L. S., Raes, D., & Smith, M. (1998). Crop evapotranspiration-Guidelines for computing crop water requirements-FAO Irrigation and drainage paper 56. *FAO, ISBN 92-5-104219-5.*

Baker, J. M., Griffis, T. J., & Ochsner, T. E. (2012). Coupling landscape water storage and supplemental irrigation to increase productivity and improve environmental stewardship in the U.S. Midwest. *Water Resources Research*, *48*(5), 2805-2814.

Blanken, P. D., Rouse, W. R., Culf, A. D., Spence, C., Boudreau, L. D., Jasper, J. N., Kochtubajda, B., Schertzer, W. M., Marsh, P., & Verseghy, D. (2000). Eddy covariance measurements of evaporation from Great Slave lake, Northwest Territories, Canada. *Water Resources Research*, *36*(4), 1069-1077.

Bonan, G. B. (1995). Sensitivity of a GCM simulation to inclusion of inland water surfaces. *Journal of Climate*, *8*(11), 2691-2704.

Brutsaert, W., & Parlange, M. B. (1998). Hydrologic cycle explains the evaporation paradox. *Nature*, *396*(6706), 30-30.

Chattopadhyay, N., & Hulme, M. (1997). Evaporation and potential evapotranspiration in India under conditions of recent and future climate change. *Agricultural and Forest Meteorology*, *87*(1), 55-73.

Cong, Z. T., Yang, D. W., & Ni, G. H. (2009). Does evaporation paradox exist in China?. *Hydrology and Earth System Sciences*, *13*(3), 357-366.

Deng, B., Liu, S., Xiao, W., Wang, W., Jin, J., & Lee, X. (2013). Evaluation of the CLM4 lake model at a large and shallow freshwater lake. *Journal of Hydrometeorology*, *14*(2), 636-649.

Downing, J. A., Prairie, Y. T., Cole, J. J., Duarte, C. M., Tranvik, L. J., Striegl, R. G., & Middelburg, J. J. (2006). The global abundance and size distribution of lakes, ponds, and impoundments. *Limnology and Oceanography*, *51*(5), 2388-2397.

Dutra, E., Stepanenko, V. M., Balsamo, G., Viterbo, P., Miranda, P., Mironov, D., & Schär, C. (2010). An offline study of the impact of lakes on the performance of the ECMWF surface scheme. *Boreal Environment Research*, *15*(2), 100-112.

Elsawwaf, M., Willems, P., Pagano, A., & Berlamont, J. (2010). Evaporation estimates from Nasser Lake, Egypt, based on three floating station data and Bowen ratio energy budget. *Theoretical & Applied Climatology*, *100*(3-4), 439-465.

Fu, G., Liu, C., Chen, S., & Hong, J. (2004). Investigating the conversion coefficients for free water surface evaporation of different evaporation pans. *Hydrological Processes*, *18*(12), 2247-2262.

Garratt, J. R. (1992). *The Atmospheric Boundary Layer*. Cambridge University Press. New York, 316 pp.

Henneman, H. E., & Stefan, H. G. (1999). Albedo models for snow and ice on a freshwater lake. *Cold Regions Science and Technology*, *29*(1), 31-48.

Hoy, R. D., & Stephens, S. K. (1977). Field Study of Evaporation- Analysis of Data From Eucumbene, Cataract, Manton and Mundaring. *Australian Water Resources Council Technical Paper*, (21).

IPCC. (2013). Climate Change 2013: The Physical Science Basis. Contribution of Working Group I to the Fifth Assessment Report of the Intergovernmental Panel on Climate Change. Cambridge University Press, New York, pp 1552.

Johnson, F., & Sharma, A. (2010). A comparison of Australian open water body evaporation trends for current and future climates estimated from Class A evaporation pans and general circulation models. *Journal of Hydrometeorology*, *11*(1), 105-121.

Jung, M., Reichstein, M., Ciais, P., Seneviratne, S. I., Sheffield, J., Goulden, M. L., Bonan, Gordon., Cescatti, A., Chen, J., Jeu, R. D., Dolman, A. J., Eugster, W., Gerten, D., Gianelle, D., Gobron, N., Heinke, J., Kimball, J., Law, B. E., Montagnani, L., Mu, Q., Mueller, B., Oleson, K., Papale, D., Richardson, A. D., Roupsard, O., Running, S., Tomelleri, E., Viovy, N., Weber, U., Williams, C., Wood, E., Zaehle, S & Zhang, K. (2010). Recent decline in the global land evapotranspiration trend due to limited moisture supply. *Nature*, *467*(7318), 951-954.

Jensen, M. E., Burman, R. D., & Allen, R. G. (1990). Evapotranspiration and irrigation water requirements. *American Society of Civil Engineers*.

Katsaros, K. B., McMurdie, L. A., Lind, R. J., & DeVault, J. E. (1985). Albedo of a water surface, spectral variation, effects of atmospheric transmittance, sun angle and wind speed. *Journal of Geophysical Research: Oceans (1978–2012)*, *90*(C4), 7313-7321.

Kendall, M. G. (1975). *Rank Correlation Methods*. Charles Griffin, London, pp 202.

Kennedy, A. D., Dong, X., Xi, B., Xie, S., Zhang, Y., & Chen, J. (2011). A comparison of MERRA and NARR reanalyses with the DOE ARM SGP data. *Journal of Climate*, *24*(17), 4541-4557.

Laird, N. F., & Kristovich, D. A. (2002). Variations of sensible and latent heat fluxes from a Great Lakes buoy and associated synoptic weather patterns. *Journal of Hydrometeorology*, *3*(1), 3-12.

Lenters, J. D., Kratz, T. K., & Bowser, C. J. (2005). Effects of climate variability on lake evaporation: Results from a long-term energy budget study of Sparkling Lake, northern Wisconsin (USA). *Journal of Hydrology*, *308*(1), 168-195.

Lee, X., Liu, S., Xiao, W., Wang, W., Gao, Z., Cao, C., Hu, C., Hu, Z., Shen, S., Wang, Y., Wen, X., Xiao, Q., Xu, J., Yang, J., & Zhang, M. (2014). The Taihu eddy flux network: An observational program on energy, water, and greenhouse gas fluxes of a large freshwater lake. *Bulletin of the American Meteorological Society*, *95*(10), 1583-1594.

Lim, W. H., & Roderick, M. L. (2012). A framework for upscaling short-term process-level understanding to longer time scales. *Hydrology & Earth System Sciences Discussions*, *9*(5).

Liu, H., Zhang, Y., Liu, S., Jiang, H., Sheng, L., & Williams, Q. L. (2009). Eddy covariance measurements of surface energy budget and evaporation in a cool season over southern open water in Mississippi. *Journal of Geophysical Research: Atmospheres*, *114*(D4), 83-84.

Mann, H. B. (1945). Nonparametric tests against trend. *Econometrica: Journal of the Econometric Society*, 13(3), 245-259.

McJannet, D. L., Cook, F. J., & Burn, S. (2013). Comparison of techniques for estimating evaporation from an irrigation water storage. *Water Resources Research*, *49*(3), 1415-1428.

Nordbo, A., Launiainen, S., Mammarella, I., Leppäranta, M., Huotari, J., Ojala, A., & Vesala, T. (2011). Long‐term energy flux measurements and energy balance over a small boreal lake using eddy covariance technique. *Journal of Geophysical Research: Atmospheres*, *116*(D2), 3-25.

Peterson, T. C., Golubev, V. S., & Groisman, P. Y. (1995). Evaporation losing its strength. *Nature*, 377(6551):687-688.

Pinker, R. T., Zhang, B., & Dutton, E. G. (2005). Do satellites detect trends in surface solar radiation? *Science*, *308*(5723), 850-854.

Priestley, C. H. B., & Taylor, R. J. (1972). On the assessment of surface heat flux and evaporation using large-scale parameters. *Monthly weather review*, *100*(2), 81-92.

Rayner, D. P. (2007). Wind run changes: the dominant factor affecting pan evaporation trends in Australia. *Journal of Climate*, *20*(14), 3379-3394.

Rienecker, M. M., Suarez, M. J., Gelaro, R., Todling, R., Bacmeister, J., Liu, E., Bosilovich, M, G., Schubert, S. D., Takacs, L., Kim, G., Bloom, S., Chen, J., Collins, D., Conaty, A., Arlindo, D. S., Gu, W., Joiner, J., Koster, R. D., Lucchesi, R., Molod, A., Owens, T., Pawson, S., Pegion. P., Redder, C. R., Reichle, R., Robertson, F. R., Ruddick, A. G., Sienkiewicz, M & Woollen, Jack. (2011). MERRA: NASA's modern-era retrospective analysis for research and applications. *Journal of Climate*, *24*(14), 3624-3648.

Rong, Y., Su, H., Zhang, R., & Duan, Z. (2013). Effects of climate variability on evaporation in Dongping Lake, China, during 2003–2010. *Advances in Meteorology*, 65(19), 153-156.

Roderick, M. L., & Farquhar, G. D. (2002). The cause of decreased pan evaporation over the past 50 years. *science*, *298*(5597), 1410-1411.

Roderick, M. L., & Farquhar, G. D. (2006). A physical analysis of changes in Australian pan evaporation. *Land & Water Australia Technical Report ANU49, The Australian National University, Canberra, Australia*.

Roderick, M. L., Rotstayn, L. D., Farquhar, G. D., & Hobbins, M. T. (2007). On the attribution of changing pan evaporation. *Geophysical research letters*, *34*(17), 251-270.

Rosenberry, D. O., Sturrock, A. M., & Winter, T. C. (1993). Evaluation of the energy budget method of determining evaporation at Williams Lake, Minnesota, using alternative instrumentation and study approaches. *Water Resources Research*, *29*(8), 2473-2483.

Rosenberry, D. O., Winter, T. C., Buso, D. C., & Likens, G. E. (2007). Comparison of 15 evaporation methods applied to a small mountain lake in the northeastern USA. *Journal of Hydrology, 340*, 149–166.

Subin, Z. M., Murphy, L. N., Li, F., Bonfils, C., & Riley, W. J. (2012a). Boreal lakes moderate seasonal and diurnal temperature variation and perturb atmospheric circulation: analyses in the Community Earth System Model 1 (CESM1). *Tellus A*, *64*(3), 53-66.

Subin, Z. M., Riley, W. J., & Mironov, D. (2012b). An improved lake model for climate simulations: model structure, evaluation, and sensitivity analyses in CESM1. *Journal of Advances in Modeling Earth Systems*, *4*(1), 183-204.

Torcellini, P. A., Long, N., & Judkoff, R. (2004). Consumptive water use for US power production. Golden: National Renewable Energy Laboratory, NREL/CP-550-35190.

Twine, T. E., Kustas, W. P., Norman, J. M., Cook, D. R., Houser, P., Meyers, T. P., Prueger, J. H., Starks, P.J., & Wesely, M. L. (2000). Correcting eddy-covariance flux underestimates over a grassland. *Agricultural and Forest Meteorology*, *103*(3), 279-300.

Walter, M. T., Wilks, D. S., Parlange, J. Y., & Schneider, R. L. (2004). Increasing evapotranspiration from the conterminous United States. *Journal of Hydrometeorology*, *5*(3), 405-408.

Wang, W., Xiao, W., Cao, C., Gao, Z., Hu, Z., Liu, S., Shen, S., Wang, L., Xiao, Q., Xu, J., Yang, D., & Lee, X. (2014). Temporal and spatial variations in radiation and energy balance across a large freshwater lake in China. *Journal of Hydrology*, *511*, 811-824.

Wang, Y., Jiang, T., Bothe, O., & Fraedrich, K. (2007). Changes of pan evaporation and reference evapotranspiration in the Yangtze River basin. *Theoretical and Applied Climatology*, *90*(1-2), 13-23.

Wild, M., Gilgen, H., Roesch, A., Ohmura, A., Long, C. N., Dutton, E. G., Forgan, B., Kallis, A., Russak, V., & Tsvetkov, A. (2005). From dimming to brightening: Decadal changes in solar radiation at Earth's surface. *Science*, *308*(5723), 847-850.

Willmott, C. J. (1981). On the validation of models. *Physical Geography*, *2*(2), 184-194.

Williamson, C. E., Saros, J. E., & Schindler, D. W. (2009). Sentinels of change. *Science (Washington)*, *323*(5916), 887-888.

Winter, T. C., Rosenberry, D. O., & Sturrock, A. M. (1995). Evaluation of 11 equations for determining evaporation for a small lake in the north central United States. *Water Resources Research*, *31*(4), 983-993.

Xu, C. Y., Gong, L., Jiang, T., Chen, D., & Singh, V. P. (2006). Analysis of spatial distribution and temporal tre nd of reference evapotranspiration and pan evaporation in Changjiang (Yangtze River) catchment. *Journal of Hy drology*, *327*(1), 81-93.

Zeng, X., Shaikh, M., Dai, Y., Dickinson, R. E., & Myneni, R. (2002). Coupling of the common land model to the NCAR community climate model. *Journal of Climate*, *15*(14), 1832-1854.

Zhao, L., Lee, X., & Liu, S. (2013). Correcting surface solar radiation of two data assimilation systems against FLUXNET observations in North America. *Journal of Geophysical Research: Atmospheres*, *118*(17), 9552-9564.

Zhu, L., Xie, M., & Wu, Y. (2010). Quantitative analysis of lake area variations and the influence factors from 1971 to 2004 in the Nam Co basin of the Tibetan Plateau. *Chinese Science Bulletin*, *55*(13), 1294-1303.

Table 1

A list of pan evaporation sites used in this study, with distance from the lake shore noted.

Site name	Pan type	Measurement period	Distance (km)
Jintan	Φ20	1971-2013	54
Changzhou	E601	1961-2013	40
Wuxi	E601	2008-2013	10
Wujiang	Φ20	1961-1988, 2001-2013	15
Changshu	Φ20	1961-2013	41
Dongshan	E601	1961-2013	2
Yixing	Φ20	1961-2013	14
Huzhou	E601	1971-2013	8

Table 2

Model bias errors in sensible (H) and latent heat flux (LE) using in-situ observation and MERRA variables as forcing inputs: ME, mean error (W m^{-2}), RMSE, root mean squares error (W m^{-2}); I, index of agreement (Willmott et al., 1981).

	MERRA forcing			In-situ forcing		
	ME	RMSE	I	ME	RMSE	I
H	3.9	12.5	0.72	1.1	9.0	0.78
LE	0.6	27.3	0.94	0.4	16.7	0.98

Table 3

Stepwise multiple regression analysis of the modeled evaporation with annual downward shortwave radiation ($S_{\downarrow}$), air temperature (T), wind speed (U), downward longwave radiation ($L_{\downarrow}$), specific humidity (q), and precipitation (P) as independent variables. All the regression coefficients are dimensionless.

	$S_{\downarrow}$	T	U	$L_{\downarrow}$	q	P	Sum
All MERRA variables							
Trend*	0.374	0.515	0.025	0.193	0.056	-0.081	
Regression coefficient	0.677	0.234	0.133	0.219	-0.379	0	
Change in Y**	0.254	0.120	0.003	0.042	-0.021	0	
Percent contribution***	60.9%	28.9%	0.8%	10.1%	-5.1%	0	95.6%
Observed U and MERRA $S_{\downarrow}$, T, $L_{\downarrow}$, q and P							
Trend*	0.374	0.515	-0.52	0.193	0.056	-0.081	
Regression coefficient	0.763	0.273	0	0	0	0	
Change in Y**	0.285	0.141	0	0	0	0	
Percent contribution***	68.5%	33.8%	0	0	0	0	102.3%

*Total change of the variable over the period 1979-2013, equal to the product of the linear regression slope and time span.

** Change in Y (lake evaporation) induced by each meteorological variable (Equation 2).

*** Percentage contribution of each meteorological variable to the observed trend in Y.

Table 4:

Stepwise multiple regression analysis of the annual pan evaporation with annual downward shortwave radiation ($S_{\downarrow}$), air temperature (T), wind speed (U), downward longwave radiation ($L_{\downarrow}$), specific humidity (q), and precipitation (P) as independent variables. Downward longwave radiation was from MERRA. While other independent variables were from actual observations. All the regression coefficients are dimensionless.

	$S_{\downarrow}$	T	U	$L_{\downarrow}$	Q	P	Sum
Observed P, q, T, U and solar (from Shanghai station) and MERRA incoming longwave radiation							
Trend*	0.256	0.738	-0.52	0.193	-0.00245	-0.0665	
Regression coefficient	0.244	0.854	0.462	-0.498	0	-0.379	
Change in Y**	0.0623	0.630	-0.240	-0.096	0	0.025	
Percent contribution***	17.3%	174.8%	-66.6%	-26.6%	0	6.9%	105.8%

*Total change of the variable over the period 1979-2013, equal to the product of the linear regression slope and time span.

** Change in Y (lake evaporation) induced by each meteorological variable (Equation 2).

*** Percentage contribution of each meteorological variable to the observed trend in Y.

Table 5:
Same as Table 4 but for the annual reference evaporation as the dependent variable.

	$S_\downarrow$	T	U	$L_\downarrow$	q	P	Sum
Trend*	0.256	0.738	-0.52	0.193	-0.00245	-0.0665	
Regression coefficient	0	0.89	0	-0.504	0	-0.251	
Change in Y**	0	0.657	0	-0.097	0	0.017	
Percent contribution***	0	113.1%	0	-16.7%	0	2.9%	99.3%

List of Figures

Figure 1: Map showing four Φ20 pan stations (black solid circle), four E601 pan stations (open circle with cross) and two EC sites (black flag: Dapukou, DPK; Bifenggang, BFG). Green color indicates Jiangsu Province and light yellow indicates Zhejiang Province.

Figure 2: Variations of annual mean MERRA meteorological variables (black lines) and actual observations (gray lines) variables from 1979 to 2013, trends for air temperature (°C $decade^{-1}$), specific humidity (kg kg^{-1} $decade^{-1}$), wind speed (m s^{-1} $decade^{-1}$), precipitation (mm $decade^{-1}$), downward longwave radiation (W m^{-2} $decade^{-1}$) and downward shortwave radiation (W m^{-2} $decade^{-1}$) are showed (3 asterisks, 2 asterisks, 1 asterisk represent trend analysis passing 99%, 95%, 90% confidence level, respectively).

Figure 3: (a-b): Time series of sensible heat (*H*) and latent heat flux (*LE*) in 2012: black line, EC observations at BFG; blue line, model calculation forced by MERRA; red line, model calculation forced by in-situ meteorology. (c-d): Comparison between model-calculated *H* and *LE* against the EC observations at BFG: open circles, model forced by MERRA meteorology; solid bullets, model forced by in-situ meteorology. Parameter bounds on the regression coefficients are for the 95% confidence interval.

Figure 4: Trends in seasonal evaporation rates calculated with the lake model and forced by the MERRA meteorology from 1979 to 2013. Solid lines are linear regression of the long-term trends.

Figure 5: Comparison of variations of annual lake evaporation: red line, lake model; and black dots and black line, average of adjusted pan evaporation for six sites (Changshu, Yixing, Jintan, Dongshan, Changzhou, Huzhou); Green dots and green line, average reference evaporation of eight weather stations surrounding the lake. Error bars are ± one standard deviation. Red dotes indicate annual evaporation from the EC observation at DPK.

Figure 6: Comparison between lake evaporation observed with EC and pan evaporation of four Φ20 pans (a-d) and four E601 pans (e-h). Each data point represents a 5-day average in 2012. The pan coefficient of each site is shown as the slope of the regression.

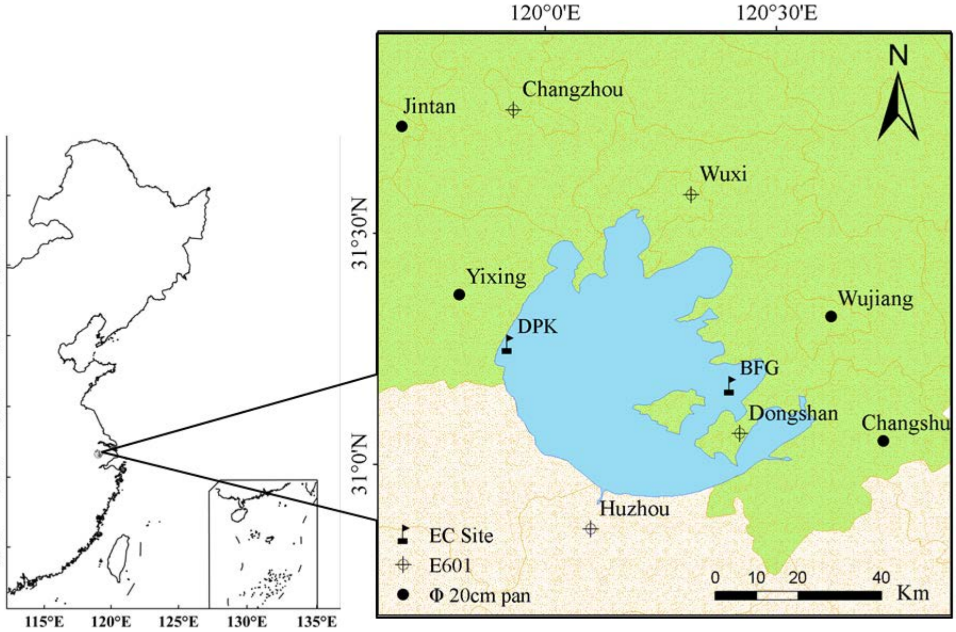

Figure 1. Map showing four Φ20 pan stations (black solid circle), four E601 pan stations (open circle with cross) and two EC sites (black flag: Dapukou, DPK; Bifenggang, BFG). Green color indicates Jiangsu Province and light yellow indicates Zhejiang Province.

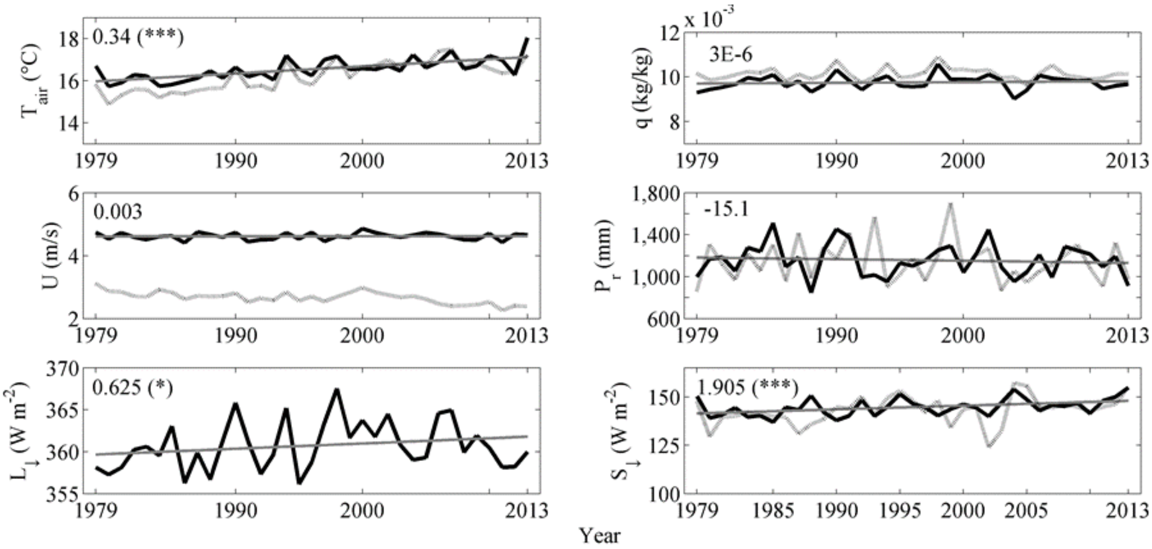

Figure 2. Variations of annual mean MERRA meteorological variables (black lines) and actual observations (gray lines) from 1979 to 2013, trends of MERRA meteorological variables for air temperature (°C decade^{-1}), specific humidity (kg kg^{-1} decade^{-1}), wind speed (m s^{-1} decade^{-1}), precipitation (mm decade^{-1}), downward longwave radiation (W m^{-2} decade^{-1}) and downward shortwave radiation (W m^{-2} decade^{-1}) are showed (3 asterisks, 2 asterisks, 1 asterisk represent trend analysis passing 99%, 95%, 90% confidence level, respectively).

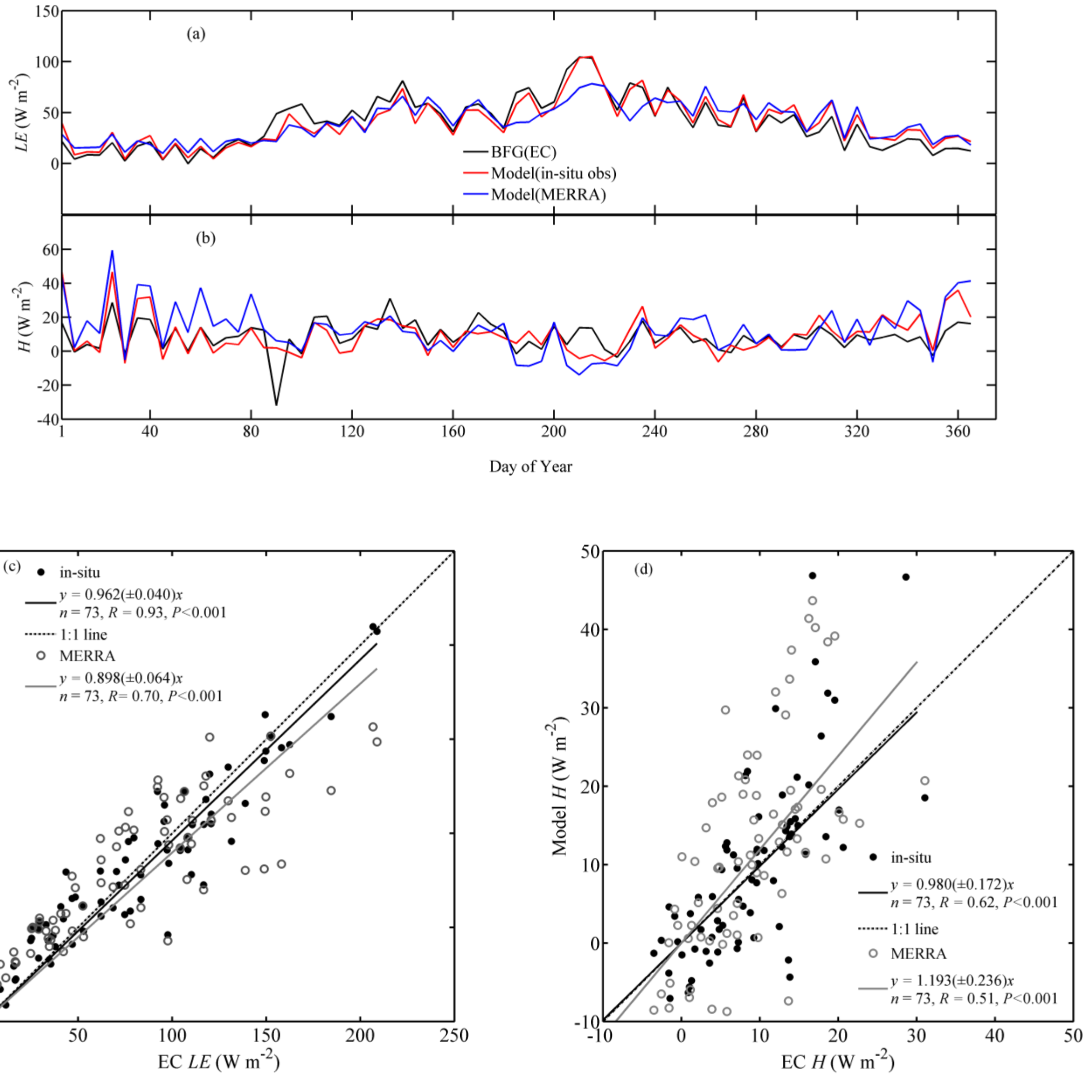

Figure 3. (a-b): Time series of sensible heat (*H*) and latent heat flux (*LE*) in 2012: black line, EC observations at BFG; blue line, model calculation forced by MERRA; red line, model calculation forced by in-situ meteorology. (c-d): Comparison between model-calculated *H* and *LE* against the EC observations at BFG: open circles, model forced by MERRA meteorology; solid bullets, model forced by in-situ meteorology. Parameter bounds on the regression coefficients are for the 95% confidence interval.

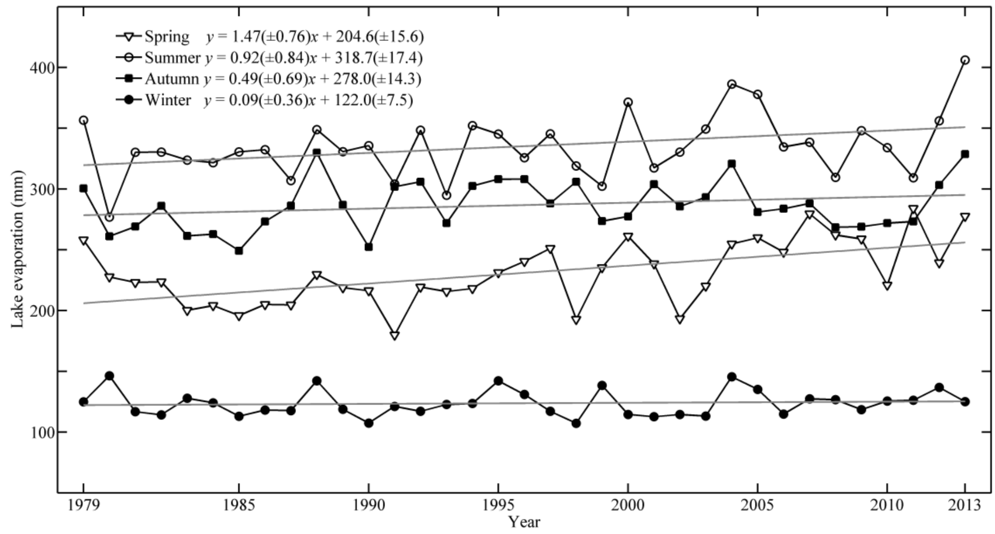

Figure 4. Trends in seasonal evaporation rates calculated with the lake model and forced by the MERRA meteorology from 1979 to 2013. Solid lines are linear regression of the long-term trends.

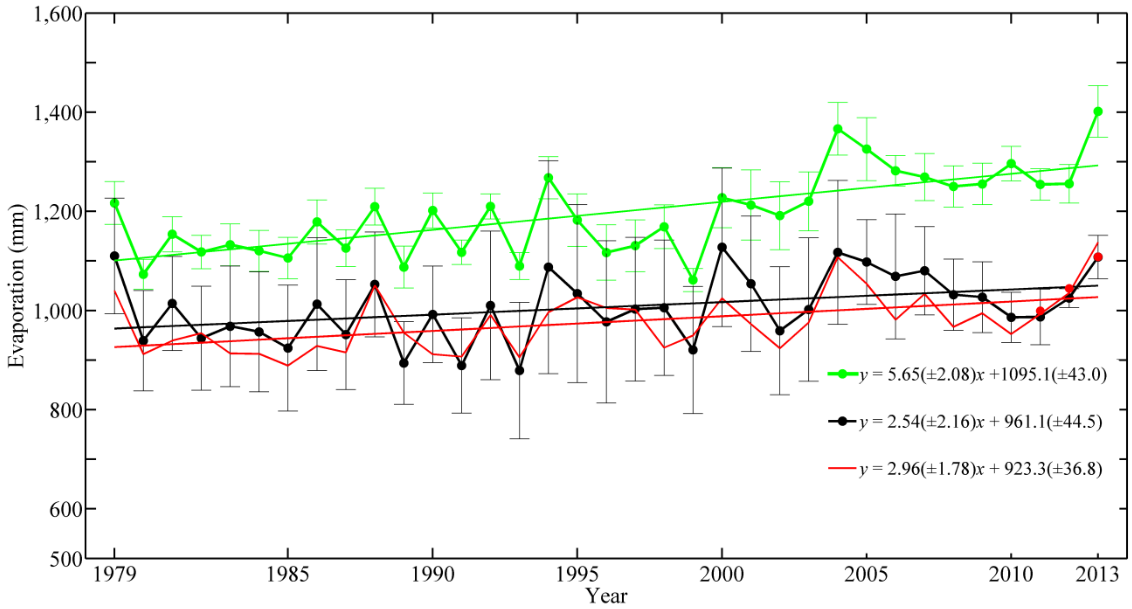

Figure 5. Comparison of variations of annual lake evaporation: red line, lake model; and black dots and black line, average of adjusted pan evaporation for six sites (Changshu, Yixing, Jintan, Dongshan, Changzhou, Huzhou); Green dots and green line, average reference evaporation of eight weather stations surrounding the lake. Error bars are ± one standard deviation. Red dotes indicate annual evaporation from the EC observation at DPK.

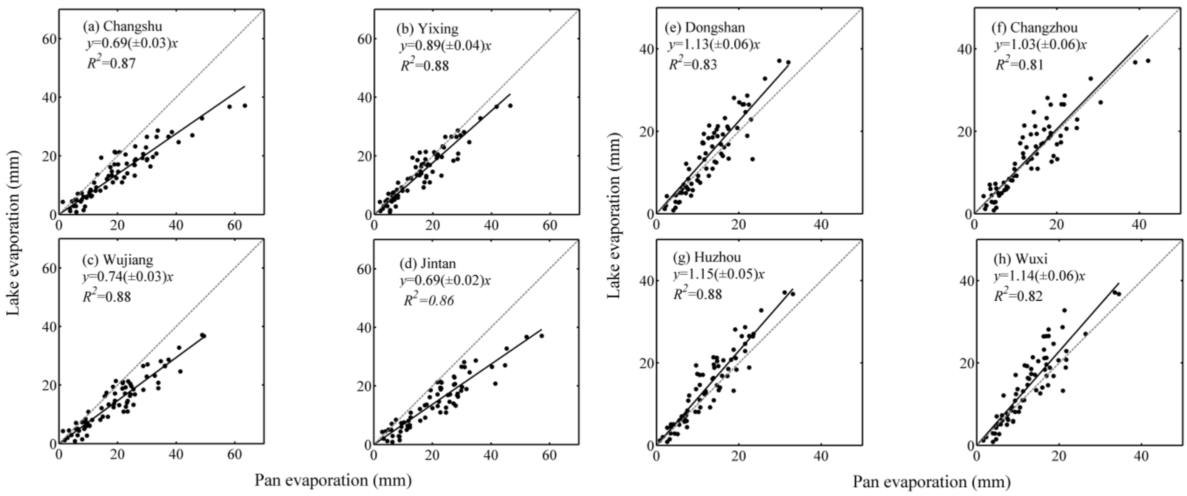

Figure 6: Comparison between lake evaporation observed with EC and pan evaporation of four Φ20 pans (a-d) and four E601 pans (e-h). Each data point represents a 5-day average in 2012. The pan coefficient of each site is shown as the slope of the regression.